8056 *Inorg. Chem.* **2010**, *49*, 8056–8066
DOI: 10.1021/ic101118y

Inorganic Chemistry
Article

Chromium−Manganese Selenide Carbonyl Complexes: Paramagnetic Clusters and Relevance to C═O Activation of Acetone

Minghuey Shieh,* Chien-Nan Lin, Chia-Yeh Miu, Miao-Hsing Hsu, Yi-Wen Pan, and Li-Fang Ho

Department of Chemistry, National Taiwan Normal University, Taipei 116, Taiwan, Republic of China

Received June 3, 2010

The paramagnetic even-electron cluster, $[Et_4N]_2[Se_2Cr_3(CO)_{10}]$, was found to react readily with $Mn(CO)_5Br$ in acetone to produce two unprecedented mixed chromium−manganese selenide carbonyl complexes, $[Et_4N][Me_2CSe_2\{Mn(CO)_4\}\{Cr(CO)_5\}_2]$ ($[Et_4N][\mathbf{1}]$) and $[Et_4N]_2[Se_2Mn_3(CO)_{10}\{Cr(CO)_5\}_2]$ ($[Et_4N]_2[\mathbf{2}]$). X-ray crystallographic analysis showed that anion **1** consisted of two Se−$Cr(CO)_5$ moieties, which were further bridged by one isopropylene group and one $Mn(CO)_4$ moiety. The dianionic cluster **2** was shown to display a Se_2Mn_3 square-pyramidal core with each Se atom externally coordinated by one $Cr(CO)_5$ group. The formation of complex **1**, presumably via C═O activation of acetone, was further facilitated by acidification of the reaction of $[Et_4N]_2[Se_2Cr_3(CO)_{10}]$ with $Mn(CO)_5Br$ in acetone. Complex **1** readily transformed into **2** upon treatment with $Mn_2(CO)_{10}$ in a KOH/MeOH/MeCN solution. Cluster **2** was a 51-electron species, which readily converted to the known 49-electron cluster $[Se_2Mn_3(CO)_9]^{2-}$ upon heating and bubbling with CO. Magnetic studies of the even-electron cluster, $[Et_4N]_2[Se_2Cr_3(CO)_{10}]$, and the odd-electron species, $[Et_4N]_2[\mathbf{2}]$ and $[PPN]_2[Se_2Mn_3(CO)_9]$, were determined by the SQUID measurement to have 2, 3, and 1 unpaired electrons, respectively. In addition, the nature and formation of complexes **1** and **2** are discussed, and the magnetic properties and electrochemistry of $[Se_2Cr_3(CO)_{10}]^{2-}$, **2**, and $[Se_2Mn_3(CO)_9]^{2-}$ were further studied and elucidated by molecular orbital calculations at the PW91 level of density functional theory.

Introduction

A variety of metal cluster complexes have been prepared in the past couple of decades,[1] and there have been great advances in their potential usages in catalysis,[2] magnetism,[3] material science, nanotechnology,[4] and most notably, in the global issue of green chemistry.[5] Recent studies have shown that bimetallic cluster complexes can be used as molecular catalysts for many industrially important reactions attributed to the synergistic interactions between two different types of metal atoms.[6,7]

Although transition metal clusters bridged by main group elements have been well studied, there has been little exploration of group 6 carbonyl chalcogenide complexes.[8−10] Compared to the larger number of main group-containing homonuclear metal clusters, there are few heteronuclear

*To whom all correspondence should be addressed. E-mail: mshieh@ntnu.edu.tw.

(1) (a) *The Chemistry of Metal Cluster Complexes*; Shriver, D. F., Kaesz, H. D., Adams, R. D., Eds.; Wiley-VCH Publishers: New York, 1990. (b) *Metal Clusters in Chemistry*; Braunstein, P., Oro, L. A., Raithby, P. R., Eds.; Wiley-VCH Publishers: New York, 1999; Vols. *1*−*3*. (c) Farrugia, L. J. *Adv. Organomet. Chem.* **1990**, *31*, 301–391. (d) Pignolet, L. H.; Aubart, M. A.; Craighead, K. L.; Gould, R. A. T.; Krogstad, D. A.; Wiley, J. S. *Coord. Chem. Rev.* **1995**, *143*, 219–263. (e) Lee, S.-M.; Wong, W.-T. *J. Cluster Sci.* **1998**, *9*, 417–444. (f) Bernardi, A.; Femoni, C.; Iapalucci, M. C.; Longoni, G.; Ranuzzi, F.; Zacchini, S.; Zanello, P.; Fedi, S. *Chem.*−*Eur. J.* **2008**, *14*, 1924–1934. (g) Adams, R. D.; Hall, M. B.; Pearl, W. C., Jr.; Yang, X. *Inorg. Chem.* **2009**, *48*, 652–662. (h) Adams, R. D.; Captain, B. *Acc. Chem. Res.* **2009**, *42*, 409–418.

(2) (a) Norton, J. H. In *Fundamental Research in Homogeneous Catalysis*; Tsutsui, M., Ugo, R., Eds.; Plenum Press: New York, 1977; Vol. *1*, p 99. (b) *Metal Clusters in Catalysis, Studies in Surface Science and Catalysis Series*; Gates, B. C., Guczi, L., Knozinger, H., Eds.; Elsevier: New York, 1986; Vol. *29*. (c) Adams, R. D. Heteronuclear Metal−Metal Bonds. In *Comprehensive Organometallic Chemistry II*; Abel, E. W., Stone, F. G. A., Wilkinson, G., Eds.; Pergamon: Oxford, 1995; Vol. *10*.

(3) (a) Kahn, O. *Molecular Magnetism*; VCH: Weinheim, 1993. (b) Mathonière, C.; Sutter, J.-P.; Yakhmi, J. V. Bimetallic magnets: Present and perspectives. In *Magnetism: molecules to materials*; Miller, J. S., Drillon, M., Eds.; Wiley-VCH: Weinheim, 2002; Vol. *4*. (c) Jensen, K. P.; Ooi, B.-L.; Christensen, H. E. M. *J. Phys. Chem. A* **2008**, *112*, 12829–12841. (d) Deng, Y.; Liu, Q.; Chen, C.; Wang, Y.; Cai, Y.; Wu, D.; Kang, B.; Liao, D.; Cui, J. *Polyhedron* **1997**, *16*, 4121–4128. (e) Prinz, M.; Kuepper, K.; Taubitz, C.; Raekers, M.; Khanra, S.; Biswas, B.; Weyhermüller, T.; Uhlarz, M.; Wosnitza, J.; Schnack, J.; Postnikov, A. V.; Schröder, C.; George, S. J.; Neumann, M.; Chaudhuri, P. *Inorg. Chem.* **2010**, *49*, 2093–2102. (f) Eichhöfer, A.; Olkowska-Oetzel, J.; Fenske, D.; Fink, K.; Mereacre, V.; Powell, A. K.; Buth, G. *Inorg. Chem.* **2009**, *48*, 8977–8984. (g) Semenaka, V. V.; Nesterova, O. V.; Kokozay, V. N.; Zybatyuk, R. I.; Shishkin, O. V.; Boca, R.; Gómez-García, C. J.; Clemente-Juan, J. M.; Jezierska, J. *Polyhedron* **2010**, *29*, 1326–1336.

(4) (a) Femoni, C.; Iapalucci, M. C.; Kaswalder, F.; Longoni, G.; Zacchini, S. *Coord. Chem. Rev.* **2006**, *250*, 1580–1604. (b) Mednikov, E. G.; Jewell, M. C.; Dahl, L. F. *J. Am. Chem. Soc.* **2007**, *129*, 11619–11630. (c) Femoni, C.; Iapalucci, M. C.; Longoni, G.; Tiozzo, C.; Zacchini, S. *Angew. Chem., Int. Ed.* **2008**, *47*, 6666–6669. (d) Anson, C. E.; Eichhöfer, A.; Issac, I.; Fenske, D.; Fuhr, O.; Sevillano, P.; Persau, C.; Stalke, D.; Zhang, J. *Angew. Chem., Int. Ed.* **2008**, *47*, 1326–1331. (e) Mednikov, E. G.; Dahl, L. F. *J. Am. Chem. Soc.* **2008**, *130*, 14813–14821. (f) Scheer, M.; Schindler, A.; Gröger, C.; Virovets, A. V.; Peresypkina, E. V. *Angew. Chem., Int. Ed.* **2009**, *48*, 5046–5049. (g) Scheer, M.; Schindler, A.; Bai, J.; Johnson, B. P.; Merkle, R.; Winter, R.; Virovets, A. V.; Peresypkina, E. V.; Blatov, V. A.; Sierka, M.; Eckert, H. *Chem.*−*Eur. J.* **2010**, *16*, 2092–2107.

Published on Web 08/03/2010

metal carbonyl clusters.[1a,b] We previously explored the chemistry of chromium carbonyl chalcogenide clusters and found it full of interest and challenge.[11] Previous studies have shown that paramagnetic metal carbonyl complexes were rare.[10c,11f,12,13] In the present study, we demonstrate the unusual reactivity exhibited by the previously reported selenium-capped trichromium cluster *closo*-$[Se_2Cr_3(CO)_{10}]^{2-}$,[11a] which is found to be paramagnetic and can readily react with $Mn(CO)_5Br$ in acetone to form novel mixed Cr−Mn selenide complexes. According to a search of the Cambridge Crystallographic Data Centre, mixed Cr−Mn selenide complexes are rare,[13e,14] and there were only five examples of Se−Cr−Mn complexes reported in the literature.

The present study provides details of the synthesis of two Cr−Mn selenide carbonyl complexes, $[Et_4N][Me_2CSe_2\{Mn(CO)_4\}\{Cr(CO)_5\}_2]$ ($[Et_4N][\mathbf{1}]$) and $[Et_4N]_2[Se_2Mn_3(CO)_{10}\{Cr(CO)_5\}_2]$ ($[Et_4N]_2[\mathbf{2}]$), from the reaction of $[Et_4N]_2[Se_2Cr_3(CO)_{10}]$ with $Mn(CO)_5Br$ in acetone, in which the former complex was formed via the C═O activation of acetone and the latter was a result of the cluster-expansion reaction. Cluster **2** was found to exhibit unusual paramagnetic properties with $S = 3/2$ at room temperature, and was further transformed to its structurally related paramagnetic cluster, $[Se_2Mn_3(CO)_9]^{2-}$, with $S = 1/2$, by bubbling with CO. In addition, the electronic, magnetic, and electrochemical properties of the even-electron complex, $[Se_2Cr_3(CO)_{10}]^{2-}$, and the odd-electron species, **2** and $[Se_2Mn_3(CO)_9]^{2-}$, were investigated and are systematically discussed with the aid of density functional theory (DFT) calculations.

Results and Discussion

Synthesis and Structures of $[Et_4N][Me_2CSe_2\{Mn(CO)_4\}\{Cr(CO)_5\}_2]$ ($[Et_4N][\mathbf{1}]$) and $[Et_4N]_2[Se_2Mn_3(CO)_{10}\{Cr(CO)_5\}_2]$ ($[Et_4N]_2[\mathbf{2}]$). Two mixed manganese−chromium selenide carbonyl complexes, $[Et_4N][Me_2CSe_2\{Mn(CO)_4\}\{Cr(CO)_5\}_2]$ ($[Et_4N][\mathbf{1}]$) and $[Et_4N]_2[Se_2Mn_3(CO)_{10}\{Cr(CO)_5\}_2]$ ($[Et_4N]_2[\mathbf{2}]$), were produced from the reaction of $[Et_4N]_2[Se_2Cr_3(CO)_{10}]$ with $Mn(CO)_5Br$ in a molar ratio 1:1.8 in an acetone solution at 35 °C with yields of 40 and 29%, respectively (Scheme 1). Compounds **1** and **2** were both characterized on the basis of IR, NMR, ICP-AES, elemental analysis, and single-crystal X-ray diffraction analysis. The existence of the two CH_3 groups of the major product **1** was confirmed by the ^1H, ^{13}C HMQC experiment, showing the ^1H NMR singlet at δ 1.82 and the ^{13}C NMR at δ 41.4. These values are in agreement with the previously

(5) (a) Dyson, P. J.; McIndoe, J. S. *Angew. Chem., Int. Ed.* **2005**, *44*, 5772–5774. (b) Hsu, M.-H.; Chen, R.-T.; Sheu, W.-S.; Shieh, M. *Inorg. Chem.* **2006**, *45*, 6740–6747. (c) Sarkar, B.; Liaw, B.-J.; Fang, C.-S.; Liu, C.-W. *Inorg. Chem.* **2008**, *47*, 2777–2785. (d) Adams, R. D.; Captain, B.; Beddie, C.; Hall, M. B. *J. Am. Chem. Soc.* **2007**, *129*, 986–1000. (e) Hassan, M. R.; Hogarth, G.; Hossain, G. M. G.; Kabir, S. E.; Raha, A. K.; Saha, M. S.; Tocher, D. A. *Organometallics* **2007**, *26*, 6473–6480. (f) Solomon, E. I.; Sarangi, R.; Woertink, J. S.; Augustine, A. J.; Yoon, J.; Ghosh, S. *Acc. Chem. Res.* **2007**, *40*, 581–591.

(6) (a) Choudhary, V. R.; Chaudhari, P. A.; Narkhede, V. S. *Catal. Commun.* **2003**, *4*, 171–175. (b) Sreekanth, P. M.; Peña, D. A.; Smirniotis, P. G. *Ind. Eng. Chem. Res.* **2006**, *45*, 6444–6449. (c) Chattopadhyay, T.; Islam, S.; Nethaji, M.; Majee, A.; Das, D. *J. Mol. Catal. A: Chem.* **2007**, *267*, 255–264. (d) Liu, X.; Henderson, J. A.; Sasaki, T.; Kishi, Y. *J. Am. Chem. Soc.* **2009**, *131*, 16678–16680. (e) Scott, R. W. J.; Sivadinarayana, C.; Wilson, O. M.; Yan, Z.; Goodman, D. W.; Crooks, R. M. *J. Am. Chem. Soc.* **2005**, *127*, 1380–1381.

(7) (a) Thomas, J. M.; Raja, R.; Lewis, D. W. *Angew. Chem., Int. Ed.* **2005**, *44*, 6456–6482. (b) Thomas, J. M.; Johnson, B. F. G.; Raja, R.; Sankar, G.; Midgley, P. A. *Acc. Chem. Res.* **2003**, *36*, 20–30. (c) Thomas, J. M.; Raja, R.; Johnson, B. F. G.; Hermans, S.; Jones, M. D.; Khimyak, T. *Ind. Eng. Chem. Res.* **2003**, *42*, 1563–1570. (d) Johnson, B. F. G. *Top. Catal.* **2003**, *24*, 147–159. (e) Thomas, J. M.; Adams, R. D.; Boswell, E. M.; Captain, B.; Grönbeck, H.; Raja, R. *Faraday Discuss.* **2008**, *138*, 301–315. (f) Adams, R. D.; Captain, B. *Angew. Chem., Int. Ed.* **2008**, *47*, 252–257. (g) Raja, R.; Adams, R. D.; Blom, D. A.; Pearl, W. C., Jr.; Gianotti, E.; Thomas, J. M. *Langmuir* **2009**, *25*, 7200–7204. (h) Van den Beuken, E. K.; Feringa, B. L. *Tetrahedron* **1998**, *54*, 12985–13011. (i) Raja, R.; Sankar, G.; Hermans, S.; Shephard, D. S.; Bromley, S.; Thomas, J. M.; Johnson, B. F. G. *Chem. Commun.* **1999**, 1571–1572. (j) Xiao, J.; Puddephatt, R. J. *Coord. Chem. Rev.* **1995**, *143*, 457–500. (k) Sivaramakrishna, A.; Clayton, H. S.; Makhubela, B. C. E.; Moss, J. R. *Coord. Chem. Rev.* **2008**, *252*, 1460–1485. (l) Alexeev, O. S.; Gates, B. C. *Ind. Eng. Chem. Res.* **2003**, *42*, 1571–1587.

(8) (a) Roof, L. C.; Kolis, J. W. *Chem. Rev.* **1993**, *93*, 1037–1080. (b) Gysling, H. J. *Coord. Chem. Rev.* **1982**, *42*, 133–244. (c) Whitmire, K. H. *Adv. Organomet. Chem.* **1998**, *42*, 1–145. (d) Mathur, P. *Adv. Organomet. Chem.* **1997**, *41*, 243–314. (e) Sekar, P.; Ibers, J. A. *Inorg. Chem.* **2002**, *41*, 450–451, and references therein. (f) Goh, L. Y. *Coord. Chem. Rev.* **1999**, *185*−*186*, 257–276. (g) Lau, H. F.; Ng, V. W. L.; Koh, L. L.; Tan, G. K.; Goh, L. Y.; Roemmele, T. L.; Seagrave, S. D.; Boeré, R. T. *Angew. Chem., Int. Ed.* **2006**, *45*, 4498–4501. (h) Lau, H. F.; Ang, P. C. Y.; Ng, V. W. L.; Kuan, S. L.; Goh, L. Y.; Borisov, A. S.; Hazendonk, P.; Roemmele, T. L.; Boeré, R. T.; Webster, R. D. *Inorg. Chem.* **2008**, *47*, 632–644.

(9) (a) Shieh, M.; Chen, P.-F.; Peng, S.-M.; Lee, G.-H. *Inorg. Chem.* **1993**, *32*, 3389–3390. (b) Shieh, M.; Tsai, Y.-C. *Inorg. Chem.* **1994**, *33*, 2303–2305. (c) Shieh, M.; Shieh, M.-H.; Tsai, Y.-C.; Ueng, C.-H. *Inorg. Chem.* **1995**, *34*, 5088–5090. (d) Shieh, M.; Tang, T.-F.; Peng, S.-M.; Lee, G.-H. *Inorg. Chem.* **1995**, *34*, 2797–2803. (e) Cherng, J.-J.; Tsai, Y.-C.; Ueng, C.-H.; Lee, G.-H.; Peng, S.-M.; Shieh, M. *Organometallics* **1998**, *17*, 255–261. (f) Huang, K.-C.; Shieh, M.-H.; Jang, R.-J.; Peng, S.-M.; Lee, G.-H.; Shieh, M. *Organometallics* **1998**, *17*, 5202–5205. (g) Shieh, M.; Chen, H.-S.; Chi, H.-H.; Ueng, C.-H. *Inorg. Chem.* **2000**, *39*, 5561–5564. (h) Lai, Y.-W.; Cherng, J.-J.; Sheu, W.-S.; Lee, G.-A.; Shieh, M. *Organometallics* **2006**, *25*, 184–190. (i) Shieh, M.; Ho, C.-H.; Sheu, W.-S.; Chen, B.-G.; Chu, Y.-Y.; Miu, C.-Y.; Liu, H.-L.; Shen, C.-C. *J. Am. Chem. Soc.* **2008**, *130*, 14114–14116. (j) Shieh, M.; Miu, C.-Y.; Lee, C.-J.; Chen, W.-C.; Chu, Y.-Y.; Chen, H.-L. *Inorg. Chem.* **2008**, *47*, 11018–11031.

(10) (a) Huang, K.-C.; Tsai, Y.-C.; Lee, G.-H.; Peng, S.-M.; Shieh, M. *Inorg. Chem.* **1997**, *36*, 4421–4425. (b) Shieh, M.; Chen, H.-S.; Yang, H.-Y.; Ueng, C.-H. *Angew. Chem., Int. Ed.* **1999**, *38*, 1252–1254. (c) Shieh, M.; Chen, H.-S.; Yang, H.-Y.; Lin, S.-F.; Ueng, C.-H. *Chem.*−*Eur. J.* **2001**, *7*, 3152–3158. (d) Shieh, M.; Hsu, M.-H. *J. Cluster Sci.* **2004**, *15*, 91–106.

(11) (a) Shieh, M.; Ho, L.-F.; Jang, L.-F.; Ueng, C.-H.; Peng, S.-M.; Liu, Y.-H. *Chem. Commun.* **2001**, 1014–1015. (b) Shieh, M.; Ho, L.-F.; Guo, Y.-W.; Lin, S.-F.; Lin, Y.-C.; Peng, S.-M.; Liu, Y.-H. *Organometallics* **2003**, *22*, 5020–5026. (c) Shieh, M.; Lin, S.-F.; Guo, Y.-W.; Hsu, M.-H.; Lai, Y.-W. *Organometallics* **2004**, *23*, 5182–5187. (d) Hsu, M.-H.; Miu, C.-Y.; Lin, Y.-C.; Shieh, M. *J. Organomet. Chem.* **2006**, *691*, 966–974. (e) Shieh, M.; Ho, L.-F.; Chen, P.-C.; Hsu, M.-H.; Chen, H.-L.; Guo, Y.-W.; Pan, Y.-W.; Lin, Y.-C. *Organometallics* **2007**, *26*, 6184–6196. (f) Shieh, M.; Chung, R.-L.; Yu, C.-H.; Hsu, M.-H.; Ho, C.-H.; Peng, S.-M.; Liu, Y.-H. *Inorg. Chem.* **2003**, *42*, 5477–5479.

(12) (a) Riccò, M.; Shiroka, T.; Carretta, S.; Bolzoni, F.; Femoni, C.; Iapalucci, M. C.; Longoni, G. *Chem.*−*Eur. J.* **2005**, *11*, 2856–2861. (b) Johnson, D. C.; Benfield, R. E.; Edwards, P. P.; Nelson, W. J. H.; Vargas, M. D. *Nature* **1985**, *314*, 231–235. (c) Albano, V. G.; Grossi, L.; Longoni, G.; Monari, M.; Mulley, S.; Sironi, A. *J. Am. Chem. Soc.* **1992**, *114*, 5708–5713. (d) Sinzig, J.; de Jongh, L. J.; Ceriotti, A.; della Pergola, R.; Longoni, G.; Stener, M.; Albert, K.; Rösch, N. *Phys. Rev. Lett.* **1998**, *81*, 3211–3214. (e) Benfield, R. E.; Edwards, P. P.; Stacy, A. M. *J. Chem. Soc., Chem. Commun.* **1982**, 525–526. (f) Teo, B. K.; DiSalvo, F. J.; Waszczak, J. V.; Longoni, G.; Ceriotti, A. *Inorg. Chem.* **1986**, *25*, 2262–2265. (g) Robinson, I.; Zacchini, S.; Tung, L. D.; Maenosono, S.; Thanh, N. T. K. *Chem. Mater.* **2009**, *21*, 3021–3026. (h) Femoni, C.; Iapalucci, M. C.; Longoni, G.; Wolowska, J.; Zacchini, S.; Zanello, P.; Fedi, S.; Riccò, M.; Pontiroli, D.; Mazzani, M. *J. Am. Chem. Soc.* **2010**, *132*, 2919–2927.

(13) (a) Cador, O.; Cattey, H.; Halet, J.-F.; Meier, W.; Mugnier, Y.; Wachter, J.; Saillard, J.-Y.; Zouchoune, B.; Zabel, M. *Inorg. Chem.* **2007**, *46*, 501–509. (b) Adams, R. D.; Miao, S.; Smith, M. D.; Farach, H.; Webster, C. E.; Manson, J.; Hall, M. B. *Inorg. Chem.* **2004**, *43*, 2515–2525. (c) Adams, R. D.; Boswell, E. M.; Captain, B.; Miao, S.; Beddie, C.; Webster, C. E.; Hall, M. B.; Dalal, N. S.; Kaur, N.; Zipse, D. *J. Organomet. Chem.* **2008**, *693*, 2732–2738. (d) Seidel, R.; Schnautz, B.; Henkel, G. *Angew. Chem., Int. Ed. Engl.* **1996**, *35*, 1710–1712. (e) Pasynskii, A. A.; Skabitski, I. V.; Torubaev, Y. V.; Semenova, N. I.; Novotortsev, V. M.; Ellert, O. G.; Lyssenko, K. A. *J. Organomet. Chem.* **2003**, *671*, 91–100. (f) Muratsugu, S.; Sodeyama, K.; Kitamura, F.; Sugimoto, M.; Tsuneyuki, S.; Miyashita, S.; Kato, T.; Nishihara, H. *J. Am. Chem. Soc.* **2009**, *131*, 1388–1389. (g) Shieh, M.; Ho, C.-H.; Sheu, W.-S.; Chen, H.-W. *J. Am. Chem. Soc.* **2010**, *131*, 4032–4033.

(14) Pasynskii, A. A.; Grigoriev, V. N.; Torubaev, Y. V.; Blokhin, A. I.; Shapovalov, S. S.; Dobrokhotova, Z. V.; Novotortsev, V. M. *Russ. Chem. Bull.* **2003**, *52*, 2689–2700.

Scheme 1

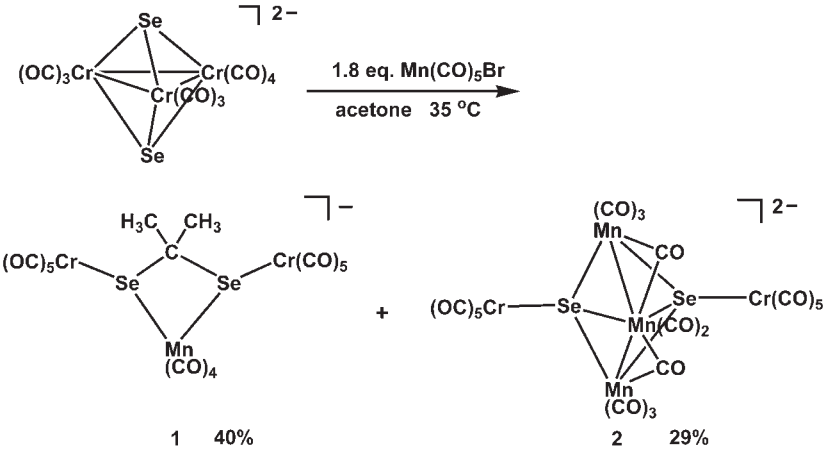

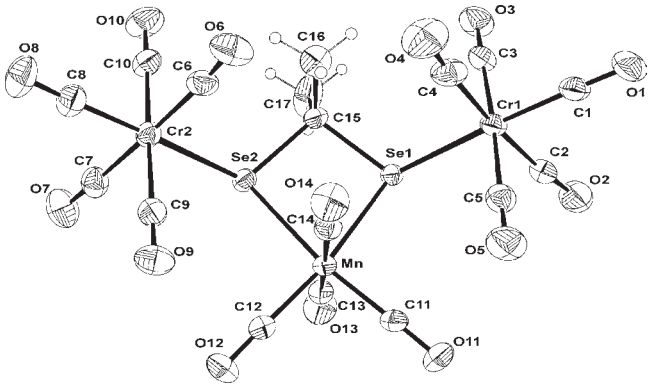

Figure 1. ORTEP diagram of anion **1**, showing 30% probability thermal ellipsoids.

reported values for $M(CO)_5(S{=}CMe_2)$ (M = Cr, Mo, W).[15] The upfield ^{13}C absorption (δ 47.1) for the quaternary carbon of the Me_2CSe_2 moiety was close to the value (δ 49.4) reported to the analogous sulfur fragment,[16] attributable to its negative natural charges (see DFT Calculations, Table 2). An Oak Ridge thermal ellipsoid plot (ORTEP) diagram of the structure of **1** is shown in Figure 1. Complex **1** was shown to have two Se atoms bridged by an isopropylene group and one $Mn(CO)_4$ fragment, to give a four-membered SeCSeMn ring in which each Se atom is externally coordinated by one $Cr(CO)_5$ fragment.

A search of the Cambridge Crystallographic Data Centre failed to identify any structurally characterized compound with a SeCSeMn ring. Complex **1** represents the first example of a SeCSeMn ring compound. Further, the Se(1)−C(15)−Se(2) and Se(1)−Mn−Se(2) bond angles were 101.2(2)° and 75.91(3)°, reflecting a strained four-membered SeCSeMn ring, with a mean deviation of 0.091 Å from the ideal plane. Surprisingly, the two $Cr(CO)_5$ moieties occupied the *syn* orientation because of the steric hindrance of the $Mn(CO)_4$ fragment. The formation of **1** is believed to have resulted from the C=O bond cleavage of acetone under our reaction conditions, which is rare in the literature. To the best of our knowledge, a related example has been observed only in the sulfur complex $W(CO)_5(S{=}CMe_2)$, which was obtained from the reaction of $W(CO)_5(SH)^-$ with ketones upon the addition of acids.[17]

Cluster **2** was a cluster-expansion product. As shown in Figure 2, the Se_2Mn_4-linked di-$Cr(CO)_5$ cluster **2**, which has a crystallographic center of symmetry at the center of the disordered Se_2Mn_4 octahedral core and a mirror plane through the $Se_2Mn(2)Mn(2a)$ base. The core geometry of **2** could be viewed as two $Cr(CO)_5$ units sandwiching a disordered Se_2Mn_4 unit in which the Mn(2) and Mn(2a) atoms are disordered and present in a 50:50 ratio. Besides, Mn(2) atom is coordinated with two terminal COs, where C(6), C(7), O(6), and O(7) atoms are also disordered with 50% occupancy. The selenium−selenium distance of 3.037(1) Å is regarded formally as nonbonding. Thus, cluster **2** can be considered to have a distorted Se_2Mn_3 square-pyramidal core with each basal Se atom bonded to one $Cr(CO)_5$ fragment. In this point of view, two basal Mn(1) and Mn(1a) atoms of the Se_2Mn_3 square-pyramidal core each had two terminal carbonyl ligands and one bridging CO, while the apical Mn(2) atom possessed two terminal carbonyl groups with two bridging COs shared with the other Mn(1) and Mn(1a) atoms, where the Se(1)−Mn(1), Se(1)−Mn(2), Se(1)−Mn(1a), Se(1a)−Mn(2) distances are 2.448(1), 2.389(2), 2.448(1), and 2.408(2) Å, while the Mn(1)−Se(1)−Mn(1a), Se(1)−Mn(1)−Se(1a), Se(1)−Mn(2)−Mn(1), Se(1a)−Mn(2)−Mn(1) angles are 103.33(4), 76.67(4), 57.54(4), and 57.35(4)°. The Se_2Mn_2 base was precisely planar and also coplanar with the pendant chromium atoms, Cr(1) and Cr(1a), which were in perfect externally bisecting positions since Mn(1)−Se(1)−Cr(1) = Mn(1a)−Se(1)−Cr(1) = 128.31(2)°.

For further comparison, the distances of the Se−Cr, Se−Mn, and Mn−Mn bonds of **1** and **2** and other related complexes are listed in Table 1. The average Se−Cr bond distance of **1** was 2.586(3) Å, which was longer than that (2.541(1) Å) of complex **2** and significantly longer than those in related complexes[11a,d,f,13e,14] (Table 1), reflecting the reactive nature of complex **1**. In complex **1**, the average Se−Mn bond was 2.5044(8) Å, comparatively longer than that in **2** (2.43(3) Å), $[Se_2Mn_3(CO)_9]^{2-}$

(15) Gingerich, R. G. W.; Angelici, R. J. *J. Organomet. Chem.* **1977**, *132*, 377–386.

(16) Windhager, J.; Görls, H.; Petzold, H.; Mloston, G.; Linti, G.; Weigand, W. *Eur. J. Inorg. Chem.* **2007**, 4462–4471.

(17) Gingerich, R. G. W.; Angelici, R. J. *J. Am. Chem. Soc.* **1979**, *101*, 5604–5608.

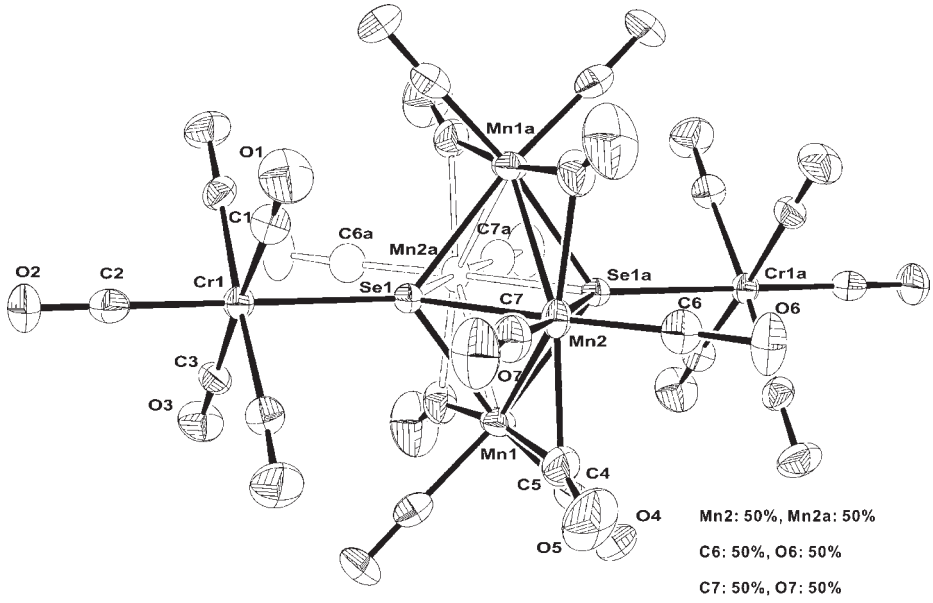

Figure 2. ORTEP diagram of anion **2**, showing 30% probability thermal ellipsoids.

Table 1. Average Bond Distances (Å) of $[Et_4N][Me_2CSe_2\{Mn(CO)_4\}\{Cr(CO)_5\}_2]$ ($[Et_4N][\mathbf{1}]$), $[Et_4N]_2[Se_2Mn_3(CO)_{10}\{Cr(CO)_5\}_2]$ ($[Et_4N]_2[\mathbf{2}]$), and Related Complexes

complex	Se−Cr	Se−Mn	Mn−Mn	ref
$[Et_4N][\mathbf{1}]$	2.586(3)	2.5044(8)		*a*
$[Et_4N]_2[\mathbf{2}]$	2.541(1)	2.43(3)	2.671(2)	*a*
$[Et_4N]_2[Se_2Cr_3(CO)_{10}]$	2.5(1)			11a
$[PPN]_2[Se_2Cr_2Fe(CO)_{10}]$	2.50(1)			11f
$[Et_4N]_2[Se_2Cr_2Mo(CO)_{10}]$	2.416(4)			11d
$[Et_4N]_2[Se_2Cr_2W(CO)_{10}]$	2.418(2)			11d
$Cp'_2Cr_2(\mu\text{-}SPh)_2(\mu_3\text{-}Se)Mn_2(CO)_9$	2.453(9)	2.5506(5)	2.9502(7)	13e
$Cp'_2Cr_2(\mu\text{-}SPh)_2(\mu_4\text{-}Se)Mn_2(CO)_8$	2.4635(7)	2.419(8)	2.835(3)	13e
$CpMnSe_2Cr(CO)_7$	2.503(2)	2.50(1)		14
$CpMnSe_2Cr_2(CO)_{12}$	2.50(1)	2.53(2)		14
$[PPh_4]_2[Se_2Mn_3(CO)_9]$		2.43(2)	2.76(6)	13d
$[PPN]_2[C_2Se_8Mn_2(CO)_6]$		2.486(9)		10a
$[PPN]_2[Se_2Mn_4(CO)_{12}]$		2.475(2)	2.705(8)	10a
$[PPh_4]_2[Mn_2(Se_4)_2(CO)_6]$		2.51(2)		18
$[Et_4N]_2[Mn(SePh)_4]$		2.567(5)		19

[a] This work.

Table 2. Results of Natural Bond Order and Natural Population Analyses of $[Se_2Cr_3(CO)_{10}]^{2-}$, **1**, **1′**, **2**, and $[Se_2Mn_3(CO)_9]^{2-}$ at the Level of PW91/LanL2DZ

	Wiberg bond index				natural charge					
complex	Se−Mn	Mn−Mn	Se−Cr	Se−C[a]	Se	Mn	Cr	C[a]	$Se_2Mn_3(CO)_x$ (sum)	$Cr_2(CO)_{10}$ (sum)
$[Se_2Cr_3(CO)_{10}]^{2-}$[b]			0.426		−0.134		−0.711			
1	0.358		0.320	0.892	0.218	−0.862	−1.332	−0.272		−0.953
1′	0.360		0.316	0.891	0.213	−0.850	−1.343	−0.266		−0.953
2	0.305	0.099	0.284		−0.028	−0.569	−1.332		−0.955 (x = 10)	−1.045
$[Se_2Mn_3(CO)_9]^{2-}$	0.423	0.116			−0.127	−0.577			−2 (x = 9)	

[a] The quaternary carbon. [b] Single-point calculations.

(2.43(2) Å),[13d] $[C_2Se_8Mn_2(CO)_6]^{2-}$ (2.486(9) Å),[10a] $[Se_2Mn_4(CO)_{12}]^{2-}$ (2.475(2) Å),[10a] and $Cp'_2Cr_2(\mu\text{-}SPh)_2(\mu_4\text{-}Se)Mn_2(CO)_8$ (2.419(8) Å)[13e] but shorter than that in $[Mn_2(Se_4)_2(CO)_6]^{2-}$ (2.51(2) Å),[18] $[Mn(SePh)_4]^{2-}$ (2.567(5) Å),[19] $Cp'_2Cr_2(\mu\text{-}SPh)_2(\mu_3\text{-}Se)Mn_2(CO)_9$ (2.5506(5) Å),[13e] and $CpMnSe_2Cr_2(CO)_{12}$ (2.53(2) Å).[14] Additionally, the average Mn−Mn bond (2.671(2) Å) of complex **2** was the shortest among the Mn−Mn bonds of the related complexes (See Table 1). Overall, the average Se−Mn and Se−Cr bond distances of **2** were shorter than the corresponding distances in **1**, suggesting stronger skeletal bonds in complex **2** versus **1**, probably because of the additional Mn−Mn bonds.

Formation of the C═O Activated Complex 1. The formation of complex **1**, via C═O activation of acetone, was further facilitated by the acidification of the reaction of $[Et_4N]_2[Se_2Cr_3(CO)_{10}]$ with $Mn(CO)_5Br$ in acetone.

(18) O'Neal, S. C.; Pennington, W. T.; Kolis, J. W. *Inorg. Chem.* **1990**, *29*, 3134–3138.
(19) Tremel, W.; Krebs, B.; Greiwe, K.; Simon, W.; Stephan, H.-O.; Henkel, G. *Z. Naturforsch.* **1992**, *47B*, 1580–1592.

Scheme 2

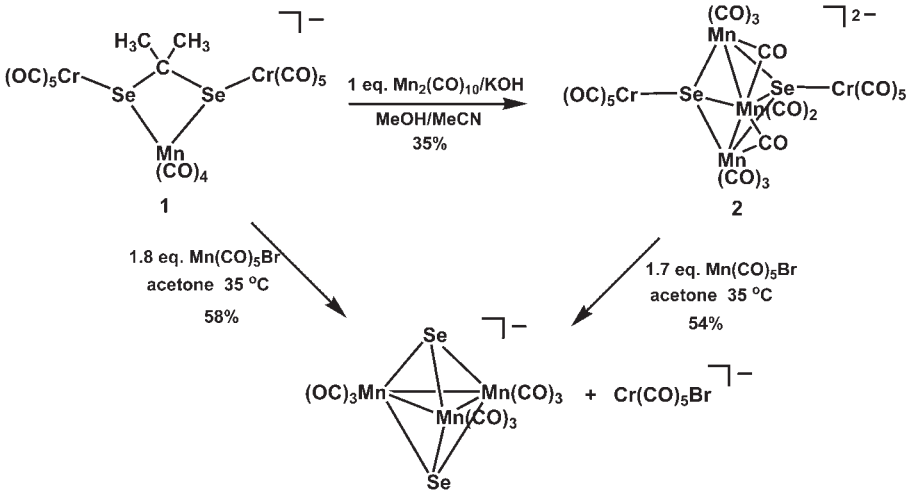

Scheme 3

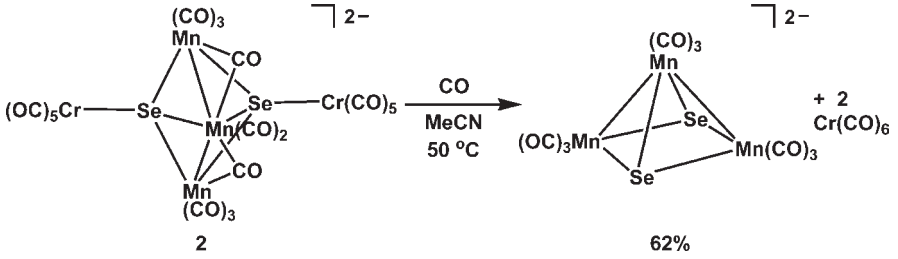

The yield of **1** increased from 40 to 61%, and the minor product **2** decreased to 12%. The formation of **1** may have occurred via the nucleophilic attack of the reactive "Se" sites of $[Se_2Cr_3(CO)_{10}]^{2-}$ on the carbon center of the acetone and the Mn atom of the incoming $[Mn(CO)_5]^+$ group, accompanied by complicated bond breakage and formation processes, to give rise to the C=O activated product **1**. The acidification of the reaction may have increased the electrophilicity of the carbon center of the acetone, and thereby enhanced the yields of complex **1**. However, the trace amount of aqueous HCl may have broken the metal skeleton of **2** to result in a decreased yield. On the other hand, we wondered whether C=O activation of the acetone analogue could be observed in the reaction of $[Se_2Cr_3(CO)_{10}]^{2-}$ with $Mn(CO)_5Br$. It turned out that when the reaction was treated with butanone under similar conditions, only complex **2** was isolated, with no observation of the C=O activation product $[Me(Et)CSe_2Cr_2Mn(CO)_{14}]^-$ (**1′**) (discussed later with DFT Calculations). Even when the reaction with butanone was acidified, the degradation product $[Se_2Mn_3(CO)_9]^-$[10a] was formed instead.

Transformation of 1 and 2. To better understand the reactivity of complexes **1** and **2**, their structural transformations were carefully examined (Scheme 2). We investigated whether complex **1** could be transformed to **2** under our reaction conditions for the reaction of $[Se_2Cr_3(CO)_{10}]^{2-}$ with $Mn(CO)_5Br$. As shown in Scheme 2, compound **1** failed to give complex **2** under the controlled conditions, but instead led to the formation of the known complexes $[Se_2Mn_3(CO)_9]^-$ and $[Cr(CO)_5Br]^-$.[10a,20] However, complex **2** was obtained from the reaction of complex **1** with $Mn_2(CO)_{10}$ in a KOH/MeOH/MeCN solution. Complex **2** also underwent cluster degradation via Se−Cr bond breakage to form $[Se_2Mn_3(CO)_9]^-$ upon its reaction with $Mn(CO)_5Br$ in acetone. These results indicate that the pathways of the formation of compounds **1** and **2** in the reaction of $[Se_2Cr_3(CO)_{10}]^{2-}$ with $Mn(CO)_5Br$ in acetone are different, and the Se−Mn bonds are stronger than the Se−Cr bonds in complexes **1** and **2** (See Table 1). This phenomenon is also supported by DFT calculations (Wiberg bond index in Table 2).

Transformation of 2 to the Paramagnetic $[Se_2Mn_3(CO)_9]^{2-}$. Complex **2** was thermally stable in refluxing MeCN solution. However, when CO was bubbled through a solution of complex **2** in MeCN at 50 °C, the known 49-electron complex, $[Se_2Mn_3(CO)_9]^{2-}$,[13d] resulted along with the formation of $Cr(CO)_6$ which was identified by IR (Scheme 3). On the basis of the result, it was believed that cluster **2** underwent two $Se-Cr(CO)_5$ bond breakage with the elimination of $Cr(CO)_6$ to give the structurally related square-pyramidal Se_2Mn_3 complex $[Se_2Mn_3(CO)_9]^{2-}$. This reaction also implied that a CO molecule was removed from the Mn_3 core to give one of the $Cr(CO)_6$ molecules. Decarbonylation reactions in anionic metal carbonyl complexes are generally quite difficult.[21]

(20) (a) Abel, E. W.; Butler, I. S.; Reid, J. G. *J. Chem. Soc.* **1963**, 2068–2070. (b) Fischer, E. O.; Öfele, K. Z. *Naturforsch.* **1959**, *14B*, 736–737. (c) Fischer, E. O.; Öfele, K. *Chem. Ber.* **1960**, *93*, 1156–1161.

(21) (a) Bernhardt, W.; Vahrenkamp, H. *Organometallics* **1986**, *5*, 2388–2389. (b) Huang, T.-K.; Chi, Y.; Peng, S.-M.; Lee, G.-H.; Wang, S.-L.; Liao, F.-L. *Organometallics* **1995**, *14*, 2164–2166.

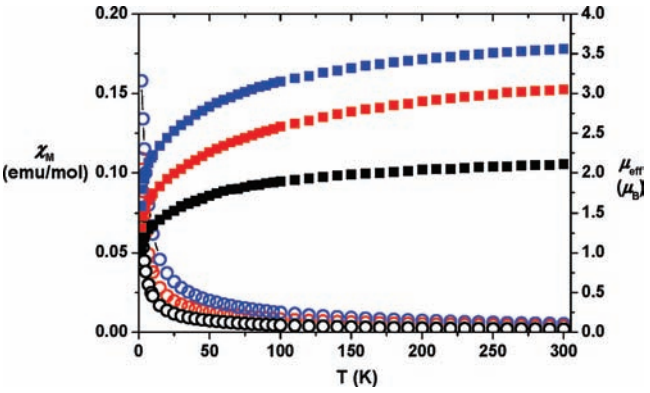

Figure 3. Temperature-dependent magnetic susceptibility data for $[Et_4N]_2[Se_2Cr_3(CO)_{10}]$ (red symbol), $[Et_4N]_2$**[2]** (blue symbol), and $[PPN]_2[Se_2Mn_3(CO)_9]$ (black symbol): χ_M vs T (○) and μ_{eff} vs T (■) plots.

Magnetic Properties of $[Et_4N]_2[Se_2Cr_3(CO)_{10}]$, $[Et_4N]_2$-[2], and $[PPN]_2[Se_2Mn_3(CO)_9]$. Although the synthesis and structure of $[Et_4N]_2[Se_2Cr_3(CO)_{10}]$ have been reported,[11a] its magnetic properties were unknown. Surprisingly, according to SQUID analysis, $[Et_4N]_2[Se_2Cr_3(CO)_{10}]$ obeyed electron-counting rules, but nonetheless exhibited paramagnetic properties. The magnetic data (see Supporting Information), in the form of χ_M versus T and μ_{eff} versus T plots for $[Et_4N]_2[Se_2Cr_3(CO)_{10}]$, are shown in Figure 3. At 300 K, $[Et_4N]_2[Se_2Cr_3(CO)_{10}]$ had the effective magnetic moment $\mu_{eff} = 3.05\,\mu_B$. This value is close to the spin-only value ($\mu_{eff} = 2.83\,\mu_B$) predicted for a simple $S = 1$ species. $[Et_4N]_2[Se_2Cr_3(CO)_{10}]$ is an electron-precise species and coordinated only with carbonyl ligands, but it is highly paramagnetic, which is an unusual phenomenon.[13g] In addition, cluster **2** is a 51-electron species, which possesses one more than the 50 electrons expected for a square-pyramidal cluster having three metals with two metal−metal bonds. Since cluster **2** is an electron-rich species, its magnetic properties were also investigated (Figure 3). The measurements showed that $[Et_4N]_2$**[2]** had an effective magnetic moment $\mu_{eff} = 3.56\,\mu_B$ at 300 K. This value is close to the spin-only value ($\mu_{eff} = 3.87\,\mu_B$) predicted for a simple $S = 3/2$ species. At low temperature, $[Et_4N]_2$**[2]** gave the $\mu_{eff} = 1.59\,\mu_B$ at 2 K, which corresponds to an $S = 1/2$ species. SQUID analysis of the 49-electron $[PPN]_2[Se_2Mn_3(CO)_9]$ was also carried out for comparison, which gave $\mu_{eff} = 2.11\,\mu_B$ at 300 K, corresponding to an $S = 1/2$ species (Figure 3). As observed in the case of $[PPh_4]_2[Se_2Mn_3(CO)_9]$,[13d] the ^{1}H NMR signals of the $[Et_4N]^+$ salt of $[Et_4N]_2[Se_2Cr_3(CO)_{10}]$, $[Et_4N]_2$**[2]**, and $[Et_4N]_2[Se_2Mn_3(CO)_9]$ were significantly broad, reflecting the paramagnetic properties of these complexes.

DFT Calculations. The DFT method was employed to develop an understanding of the nature of $[Se_2Cr_3(CO)_{10}]^{2-}$, **1**, **2**, and $[Se_2Mn_3(CO)_9]^{2-}$ to rationalize their transformation behaviors. All the calculations were carried out at the PW91[22,23]/LanL2DZ level of theory. The geometry of $[Se_2Cr_3(CO)_{10}]^{2-}$ was taken from single-crystal diffraction data,[11a] and the geometries of **1**, **2**, and $[Se_2Mn_3(CO)_9]^{2-}$ were optimized with the same level of theory. On the basis of the single-crystal diffraction data of complex **1**, the isopropylene group of complex **1** was replaced by the *sec*-butylene group, forming the proposed structure $[Me(Et)CSe_2Cr_2Mn(CO)_{14}]^-$ (**1′**), which was also fully optimized with the same level of theory. In addition, the Wiberg bond indices[24] and natural population analyses (NPA)[25] for $[Se_2Cr_3(CO)_{10}]^{2-}$, **1**, **1′**, **2**, and $[Se_2Mn_3(CO)_9]^{2-}$ were calculated, and the results are further analyzed and listed in Table 2.

The calculated results reveal that the active sites of the paramagnetic $[Se_2Cr_3(CO)_{10}]^{2-}$ for the formation of complexes **1** and **2** could be related to the higher singly occupied molecular orbital (SOMO) of $[Se_2Cr_3(CO)_{10}]^{2-}$. As shown in Figure 4, the higher-energy SOMO of $[Se_2Cr_3(CO)_{10}]^{2-}$ had a significant contribution from the d orbitals of the Cr atoms, each attached to three COs, and the p orbitals of the Se atoms. Thus, it is proposed that the less hindered "Se" sites of $[Se_2Cr_3(CO)_{10}]^{2-}$ could undergo nucleophilic attack onto the carbon center of the acetone or/and the incoming $[Mn(CO)_5]^+$ fragment, accompanied by complicated Se−Cr and Cr−Cr bond breakage and Se−C and Se−Mn or Mn−Mn formation, to give rise to the formation of complex **1** or **2**. In addition, natural population analyses show that the Se atoms in complex **1** or **2** became more positively charged (0.218 or −0.028) than those in $[Se_2Cr_3(CO)_{10}]^{2-}$ (−0.134), which accounts for the dispersed electron density of Se atoms onto additional Mn and Cr atoms. It is noted that the Se−Cr bonds are weaker than the Se−Mn bonds in **1** and **2**, which is consistent with the calculated Wiberg bond indices (0.320 vs 0.358 and 0.284 vs 0.305) (Table 2). Moreover, the Wiberg bond indices for the Se−C bonds (0.892) in the SeCSeMn ring of **1** were significantly greater than Se−Mn (0.358) and Se−Cr (0.320) bonds, indicative of stronger Se−C bonds, which should contribute to the stability of the SeCSeMn ring in the C═O activated complex **1**. Therefore, the Se−C fragments played an important role in stabilizing complex **1**.

The optimized structure of the proposed complex $[Me(Et)CSe_2\{Mn(CO)_4\}\{Cr(CO)_5\}_2]^-$ (**1′**) was calculated to understand why this complex was not found in the reaction of $[Se_2Cr_3(CO)_{10}]^{2-}$ with $Mn(CO)_5Br$ in butanone. The Wiberg bond indices and natural population analyses (NPA) for complexes **1** and **1′** were also compared (see Table 2). The calculations showed that the corresponding Wiberg bond indices for **1** and **1′** were similar. In addition, each Se atom in **1** and **1′** carried slight positive charges (0.218, 0.213), while the bridging C atom carried −0.272 and −0.266, respectively, indicative of the comparative Coulomb force of the Se−C bonds in **1** and **1′**. These results indicate that the thermal stability of **1** and **1′** is similar, which contrasted with the experimental results that the analogous C═O activated product in butanone was not observed under our reaction conditions. Therefore, the failure to produce complex **1′** was probably due to the large steric repulsion between the *sec*-butylene group and carbonyls of the $Cr(CO)_5$ fragment (See Supporting Information, Figure S1).

(22) Burke, K.; Perdew, J. P.; Wang, Y. In *Electronic Density Functional Theory: Recent Progress and New Directions*; Dobson, J. F., Vignale, G., Das, M. P., Eds.; Plenum: New York, 1998.
(23) (a) Perdew, J. P. *Phys. Rev. B.* **1986**, *33*, 8822–8824. (b) Perdew, J. P.; Wang, Y. *Phys. Rev. B.* **1992**, *45*, 13244–13249.
(24) Wiberg, K. B. *Tetrahedron* **1968**, *24*, 1083–1096.
(25) (a) Reed, A. E.; Weinhold, F. *J. Chem. Phys.* **1983**, *78*, 4066–4073. (b) Reed, A. E.; Weinstock, R. B.; Weinhold, F. *J. Chem. Phys.* **1985**, *83*, 735–746.

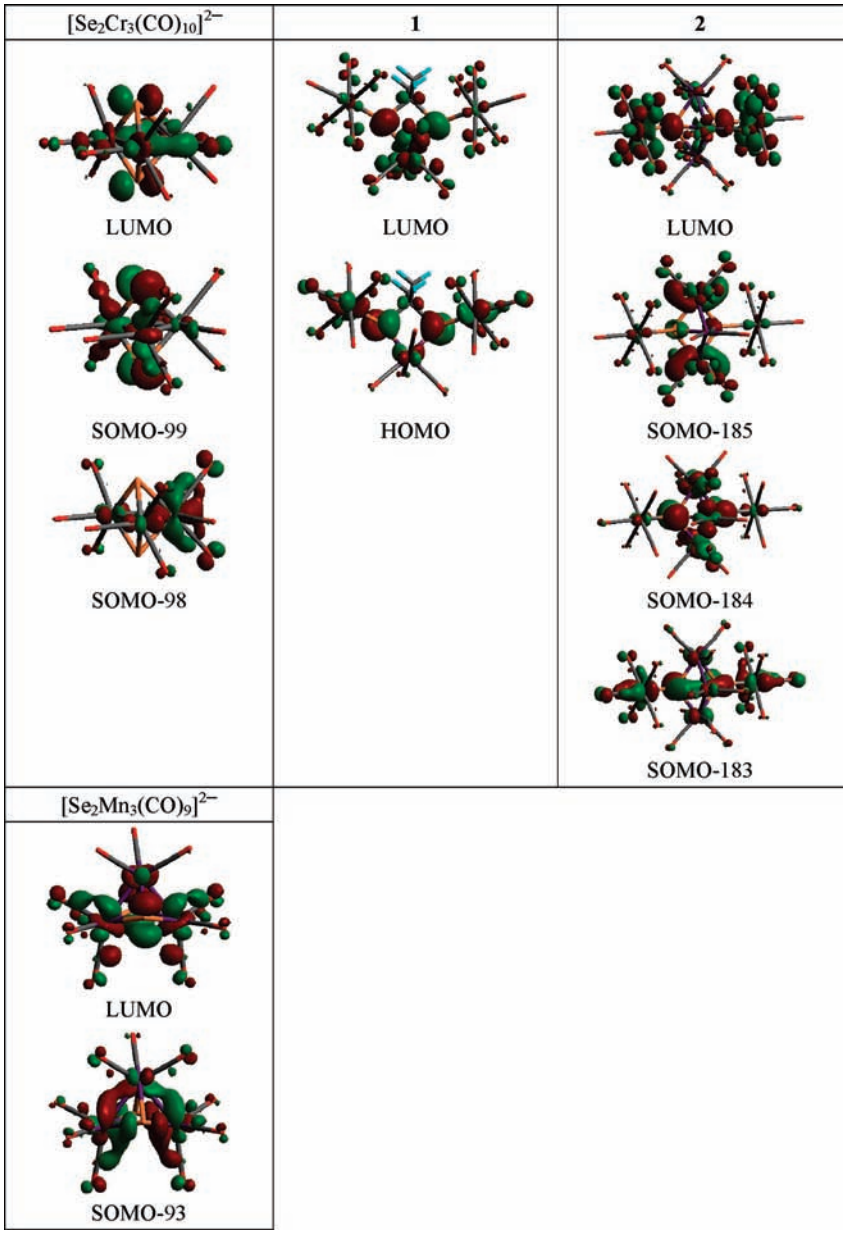

Figure 4. Spatial graphs (isovalue = 0.03−0.04) of selected frontier molecular orbitals of $[Se_2Cr_3(CO)_{10}]^{2-}$, **2**, and $[Se_2Mn_3(CO)_9]^{2-}$.

The active sites for the reaction of compound **1** with $Mn_2(CO)_{10}$/KOH to give complex **2** may, furthermore, be related to the lowest unoccupied molecular orbital (LUMO) of complex **1**. As shown in Figure 4, the LUMO of **1** received a significant contribution from the d orbitals of the Mn atom and the s and p orbitals of the Se atoms. It is reasonable to suggest that the incoming Mn-anions could interact with the Mn and Se atoms of complex **1**, accompanied by Se−CMe_2 bond breakage and Se−Mn and Mn−Mn bond formation, to produce complex **2**. Finally, $\Delta G = -16.36$ and $\Delta E = -1.33$ kcal/mol were calculated for the reaction of **2** with CO to give $[Se_2Mn_3(CO)_9]^{2-}$. In this case, the LUMO of complex **2** received major contributions from the s and p orbitals of the Se atoms and p and d orbitals of the Cr atoms (Figure 4), indicating that CO can nucleophilically attack the "Se−Cr" bonds of complex **2** to induce Se−Cr bond breakage to give $Cr(CO)_6$ and $[Se_2Mn_3(CO)_9]^{2-}$.

Spin Density Distribution of $[Se_2Cr_3(CO)_{10}]^{2-}$, 2, and $[Se_2Mn_3(CO)_9]^{2-}$. To better understand the magnetic properties of paramagnetic $[Se_2Cr_3(CO)_{10}]^{2-}$, **2**, and $[Se_2Mn_3(CO)_9]^{2-}$, the spin population of each complex was calculated, and the results are summarized in Table 3. As shown in Figure 5, the spin density of $[Se_2Cr_3(CO)_{10}]^{2-}$ was highly concentrated around the central Cr_3 ring (1.370), but with uneven delocalization[26] around three Cr atoms (0.118, Cr2; 0.626, Cr3; 0.626, Cr13), where Cr3 and Cr13 are coordinated with three COs and Cr2 is bonded to four COs. This is parallel to the probability density distribution predicated from the SOMOs of $[Se_2Cr_3(CO)_{10}]^{2-}$. It is of interest that the spin densities of cluster **2** and $[Se_2Mn_3(CO)_9]^{2-}$ were mostly concentrated on the Mn atoms (2.581 and 0.873, respectively), and an increasing population of Mn atoms in cluster **2** versus

(26) Koukaras, E. N.; Zdetsis, A. D. *Organometallics* **2009**, *28*, 4308–4315.

Table 3. Calculated Mulliken Spin Density for $[Se_2Cr_3(CO)_{10}]^{2-}$ (S = 1), **2** (S = 3/2), and $[Se_2Mn_3(CO)_9]^{2-}$ (S = 1/2) at the Level of PW91/LanL2DZ

complex	atom	total spin density	atom	spin density[a]
$[Se_2Cr_3(CO)_{10}]^{2-}$[b]	Se	0.500	Se1	0.250
			Se12	0.250
	Cr	1.370	Cr2	0.118
			Cr3	0.626
			Cr13	0.626
	CO for Cr	0.129	C	−0.007
			O	0.136
2	Se	0.150	Se1	0.075
			Se19	0.075
	Mn	2.581	Mn2	0.596
			Mn3	1.389
			Mn22	0.596
	Cr	0.118	Cr4	0.059
			Cr27	0.059
	CO for Mn	0.071	C	−0.034
			O	0.105
	CO for Cr	0.079	C	0.037
			O	0.042
$[Se_2Mn_3(CO)_9]^{2-}$	Se	0.092	Se3	0.052
			Se4	0.040
	Mn	0.873	Mn1	0.393
			Mn2	0.096
			Mn9	0.384
	CO for Mn	0.035	C	0.019
			O	0.016

[a] The negative values represent the β spin density. [b] Single-point calculations.

$[Se_2Mn_3(CO)_9]^{2-}$ was noted as the additional two $Cr(CO)_5$ units and one CO were introduced. Further, the net spin densities of COs in **2** revealed that significant overlaps between the 3d orbitals of Mn atoms and 3σ orbitals of COs occurred and gave rise to spin pairing. The uneven spin densities around the central Mn_3 core were also found for complexes **2** and $[Se_2Mn_3(CO)_9]^{2-}$ (complex **2**: 1.389, Mn3; 0.596, Mn2; 0.596, Mn22; $[Se_2Mn_3(CO)_9]^{2-}$: 0.096, Mn2; 0.393, Mn1; 0.384, Mn9), suggesting that the Mn_3 atoms may play an important role in further reactivity.

The calculations show that complex **2** with one unpaired electron was more stable than **2** with three unpaired electrons, by −41.05 kcal/mol at 0 K in the gas phase (single-point energy calculated by PW91/LanL2DZ). In addition, the optimized **2** with one unpaired electron was also more stable than the configuration with three unpaired electrons by $\Delta G = -26.26$ and $\Delta E = -28.35$ kcal/mol at the same level of calculation. These results are consistent with the experimentally determined magnetic data for **2** at 2 K (μ_{eff} = 1.59 μ_B). However, the experimental studies indicate that complex **2** converted into its high-spin state (S = 3/2) at 300 K (μ_{eff} = 3.56 μ_B). Thus, the higher paramagnetism of complex **2** at 300 K might be explained by the thermal excitation[3a] of the paired electrons into the unpaired ones. As shown in Supporting Information, Figure S2, it is interesting to note that a substantial alternation in the orbital coefficients of the Mn atoms of the three SOMOs was observed. The calculations showed that the contribution from the d and p orbitals of the Mn atoms of the SOMOs was in increasing order of SOMO-183 < SOMO-184 < SOMO-185 for complex **2** with three unpaired electrons (see Figure 4 and Supporting Information, Table S4). In addition, the energy gap between SOMO-185 and SOMO-184 was smaller than that between SOMO-184 and SOMO-183 (see Supporting Information, Figure S2). The small energy gap and the increasing contribution of Mn atoms for the two near SOMO-184 and SOMO-185 orbitals might suggest spin-pairing for complex **2** at low temperature. Moreover, the energy gap between LUMO and the highest SOMO (SOMO-185) of complex **2** was about 0.84 eV, while the energy difference between LUMO and SOMO for complex $[Se_2Mn_3(CO)_9]^{2-}$ was calculated to be 1.40 eV. Complex **2** can be regarded as being composed of the core complex $[Se_2Mn_3(CO)_9]^{2-}$ with an additional CO on the Mn atoms and the two Se atoms externally bonded with two $Cr(CO)_5$ units, and therefore the energy gaps for **2** would diminish with the increase in effective magnetic moment, compared with $[Se_2Mn_3(CO)_9]^{2-}$. These results suggest that a progressive tightening of the frontier energy levels as a function of the size of the metal clusters could trigger magnetism in complexes with an increasing number of metals.[12a]

Electrochemistry of $[Et_4N]_2[Se_2Cr_3(CO)_{10}]$, $[Et_4N]_2$[2], and $[PPN]_2[Se_2Mn_3(CO)_9]$. In view of the interesting paramagnetism and the structural relationship among $[Et_4N]_2[Se_2Cr_3(CO)_{10}]$, $[Et_4N]_2$[**2**], and $[PPN]_2[Se_2Mn_3(CO)_9]$, the electrochemical behavior of these three complexes was further investigated using cyclic voltammetry (CV) and differential pulse voltammetry (DPV) in MeCN (Figure 6, Supporting Information, Figure S3, Table 4, and Supporting Information, Table S5). Because of the interference of $[Et_4N]^+$ and $[PPN]^+$, the scan range was set between ∼1.00 to ∼ −1.00 V for these studies.

As shown in Figure 6, the CV of $[Et_4N]_2[Se_2Cr_3(CO)_{10}]$ exhibited two broad anodic peaks around ∼0.458 and ∼ −0.147 V, which were further resolved by the DPV study to have four quasi-reversible redox couples (E_p^{red} = 0.371 V, $W_{1/2}$ = 140 mV; E_p^{red} = 0.067 V, $W_{1/2}$ = 103 mV; E_p^{red} = −0.037 V, $W_{1/2}$ = 102 mV; E_p^{red} = −0.189 V, $W_{1/2}$ = 133 mV). The SOMOs of $[Se_2Cr_3(CO)_{10}]^{2-}$ received a significant contribution from the d orbitals of Cr_3 atoms (Figure 4), indicating that the rich redox reactions mainly occurred in the central Cr_3 ring. On the other hand, the CV of **2** exhibited broad anodic peaks around ∼0.439 and ∼0.182 V, which were further confirmed by DPV to have three redox couples (E_p^{red} = 0.464 V, $W_{1/2}$ = 86 mV; E_p^{red} = 0.368 V, $W_{1/2}$ = 106 mV; E_p^{red} = 0.160 V, $W_{1/2}$ = 138 mV). In addition, $[PPN]_2[Se_2Mn_3(CO)_9]$ displayed three broad oxidation peak around ∼0.591 V, ∼ −0.051 and ∼ −0.210 V, which were further confirmed by DPV (E_p^{red} = 0.572 V, $W_{1/2}$ = 106 mV; E_p^{red} = −0.105 V, $W_{1/2}$ = 99 mV; E_p^{red} = −0.273 V, $W_{1/2}$ = 109 mV), indicating three one-electron quasi-reversible redox couples. These results indicated that a similar type, with three redox couples, was observed for complex **2** and the related $[Se_2Mn_3(CO)_9]^{2-}$. The explanation may be that the SOMOs of **2** and the LUMO and SOMO of $[Se_2Mn_3(CO)_9]^{2-}$ each received a significant contribution from the d orbitals of Mn_3 atoms (Figure 4), indicating the redox reactions mainly occurred in the Mn_3 atoms. DPV further showed that the three quasi-reversible redox couples of **2** were, in general, shifted to more positive potentials than those of $[Se_2Mn_3(CO)_9]^{2-}$, which indicated that **2** was easier to be reduced, but more difficult to be oxidized because of the two attached electron-withdrawing $Cr(CO)_5$ fragments. Furthermore, as shown in Table 2, the natural charges for each $Se_2Mn_3(CO)_x$ core in $[Se_2Mn_3(CO)_9]^{2-}$ and **2** were decreasing in negative

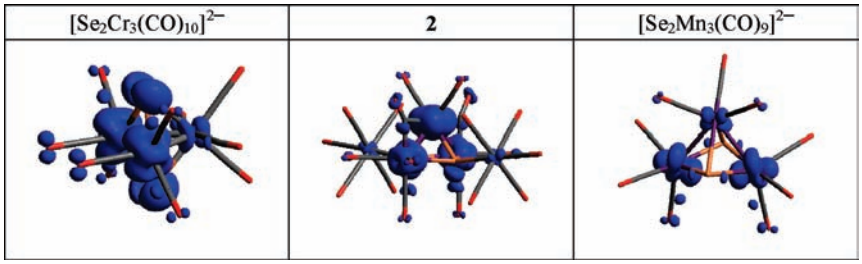

Figure 5. Spatial graphs (isovalue = 0.004) of the electron spin density of $[Se_2Cr_3(CO)_{10}]^{2-}$, **2**, and $[Se_2Mn_3(CO)_9]^{2-}$.

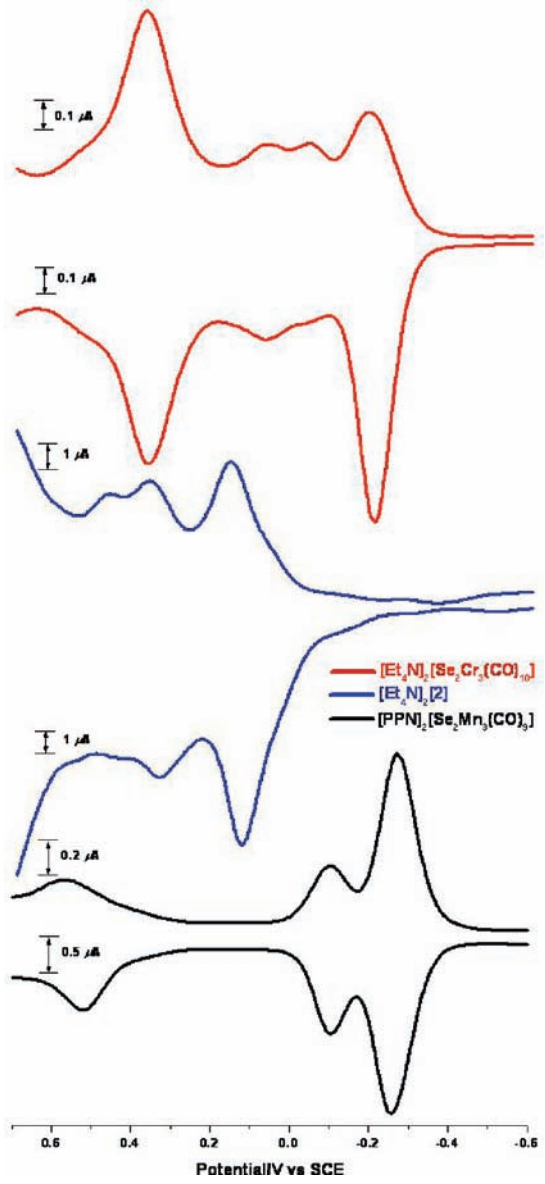

Figure 6. DPVs in MeCN for $[Et_4N]_2[Se_2Cr_3(CO)_{10}]$ (red), $[Et_4N]_2$[**2**] (blue), and $[PPN]_2[Se_2Mn_3(CO)_9]$ (black). Conditions: electrolyte, 0.1 M Bu_4NClO_4; working electrode, platinum disk; scan rate, 100 mV s^{-1}. Potentials are versus SCE.

values, indicating the electron-withdrawing effect of the $Cr(CO)_5$ fragments.

Summary

We have discovered a new series of mixed chromium−manganese selenide carbonyl complexes from the reaction of the paramagnetic cluster $[Et_4N]_2[Se_2Cr_3(CO)_{10}]$ with $Mn(CO)_5Br$ in acetone, in which a novel C=O activation complex **1** and an unusual paramagnetic cluster **2** were obtained. Cluster **2** can react with CO to produce a structurally related cluster $[Se_2Mn_3(CO)_9]^{2-}$. Surprisingly, SQUID analysis showed that the even-electron complex, $[Se_2Cr_3(CO)_{10}]^{2-}$, and the odd-electron species, **2** and $[Se_2Mn_3(CO)_9]^{2-}$, possess 2, 3, and 1 unpaired electrons, respectively. Furthermore, the electrochemical studies showed an anodic shift for the redox couples of complex **2** compared with those of its related cluster $[Se_2Mn_3(CO)_9]^{2-}$ that can be attributed to the electron-withdrawing effect of the externally bonded $Cr(CO)_5$ fragments, which was supported by theoretical calculations.

Table 4. Differential Pulse Voltammetry of $[Et_4N]_2[Se_2Cr_3(CO)_{10}]$, $[Et_4N]_2$[**2**], and $[PPN]_2[Se_2Mn_3(CO)_9]$

	oxidation process		reduction process	
compound	E_p^{ox}/V^a	E_p^{red}/V^b	E_p^{ox}/V^a	E_p^{red}/V^b
$[Et_4N]_2[Se_2Cr_3(CO)_{10}]$	0.367	0.371	−0.029	−0.037
	0.067	0.067	−0.201	−0.189
$[Et_4N]_2$[**2**]	0.428	0.464		
	0.340	0.368		
	0.132	0.160		
$[PPN]_2[Se_2Mn_3(CO)_9]$	0.520	0.572	−0.105	−0.105
			−0.257	−0.273

[a] E_p^{ox} = oxidative peak potential. [b] E_p^{red} = reductive peak potential.

Experimental Section

All reactions were performed under an atmosphere of pure nitrogen using standard Schlenk techniques.[27] Solvents were purified, dried, and distilled under nitrogen prior to use. $Mn(CO)_5Br$ (Strem), $Mn_2(CO)_{10}$ (Strem), and KOH (Showa) were used as received. Compound $[Et_4N]_2[Se_2Cr_3(CO)_{10}]$ was prepared according to the published method.[11a] Infrared spectra were recorded on a Perkin-Elmer Paragon 500 IR spectrometer as solutions in CaF_2 cells. The NMR spectra were obtained on a Bruker AV 400 at 400.13 MHz for ^1H and 100.61 MHz for ^{13}C or on a Bruker AV 500 at 500.13 MHz for ^1H and 125.76 MHz for ^{13}C. HMQC (heteronuclear multiple quantum coherence) was performed by using standard Bruker pulse sequences. ^1H and ^{13}C chemical shifts are reported in parts per million and were calibrated relative to DMSO-d_6 (^1H: 2.49 ppm, ^{13}C: 39.5 ppm) or acetone-d_6 (^1H: 2.05 ppm, ^{13}C: 29.92, 206.68 ppm) as the internal standard. FAB mass spectra were produced using a JEOL SX-102A mass spectrometer. Elemental analyses for C, H, and N were performed on a Perkin-Elmer 2400 analyzer at the NSC Regional Instrumental Center at National Taiwan University, Taipei, Taiwan. The manganese and chromium contents of complexes **1** and **2** were determined with an inductively coupled

(27) Shriver, D. F.; Drezdon, M. A. *The Manipulation of Air-Sensitive Compounds*; Wiley-VCH Publishers: New York, 1986.

plasma-atomic emission (ICP-AES) spectrometer (Perkin-Elmer Optima 3000DV) at the NSC Regional Instrumental Center at National Tsing Hua University, Hsinchu, Taiwan.

The magnetic susceptibility of the compounds was measured in gelatin capsules from 2 to 300 K in a magnetic field of 10,000 G using a Quantum Design MPMS5 SQUID magnetometer. Electrochemical measurements were performed at room temperature under a nitrogen atmosphere and recorded using a BAS-100W and CHI 621D electrochemical potentiostat. A platinum disk working electrode, a platinum wire auxiliary electrode, and a non-aqueous Ag/Ag^+ electrode were used in a three-electrode configuration. Tetra-*n*-butylammonium perchlorate (TBAP) was used as the supporting electrolyte, and the solute concentration was $\sim 10^{-3}$ M. The redox potentials were calibrated with a ferrocenium/ferrocene (Fc^+/Fc) couple in the working solution.

Synthesis of $[Et_4N][Me_2CSe_2\{Mn(CO)_4\}\{Cr(CO)_5\}_2]$ ($[Et_4N][\mathbf{1}]$) and $[Et_4N]_2[Se_2Mn_3(CO)_{10}\{Cr(CO)_5\}_2]$ ($[Et_4N]_2[\mathbf{2}]$). Method 1. An acetone solution (30 mL) of $[Et_4N]_2[Se_2Cr_3(CO)_{10}]$ (0.64 g, 0.75 mmol) and $Mn(CO)_5Br$ (0.38 g, 1.38 mmol) was stirred at 35 °C for 10 h. The solution was filtered, and the solvent was evaporated under vacuum. The residue was washed several times with hexanes and extracted with Et_2O to give a reddish-orange solution, which was recrystallized with hexanes/Et_2O to give $[Et_4N][Me_2CSe_2\{Mn(CO)_4\}\{Cr(CO)_5\}_2]$ ($[Et_4N][\mathbf{1}]$) (yield 0.26 g, 0.30 mmol, 40% based on $[Et_4N]_2[Se_2Cr_3(CO)_{10}]$). IR ($\nu_{CO}$, CH_2Cl_2): 2072 (w), 2050 (m), 1989 (s, br), 1930 (vs), 1889 (m, br) cm^{-1}. Anal. Calcd for $[Et_4N]_2[\mathbf{1}]$: C, 34.07; H, 2.97; N, 1.59. Found: C, 33.74; H, 2.98; N, 1.55. ICP-AES: Mn: Cr = 1: 1.93. Negative ion FAB MS: *m*/*z* 752.96 (calcd: 753). ^{1}H NMR (500 MHz, acetone-d_6, 300 K): δ 1.41 (t, $-CH_2CH_3$), 1.82 (s, $-CH_3$), 3.51 (q, $-CH_2CH_3$). ^{13}C NMR (125 MHz, acetone-d_6, 300 K): δ 7.76 ($-CH_2CH_3$), 41.4 ($-CH_3$), 47.1 ($-CMe_2$), 53.1 ($-CH_2CH_3$), 212.9, 218.2, 218.7, 219.6, 220.1, 223.9, 225.0 ($-CO$). Crystals of $[Et_4N][\mathbf{1}]$ suitable for X-ray diffraction were grown from Et_2O. The residue was extracted with CH_2Cl_2 to give a yellowish-brown solution, which and then with Et_2O/CH_2Cl_2 to give $[Et_4N]_2[Se_2Mn_3(CO)_{10}\{Cr(CO)_5\}_2]$ ($[Et_4N]_2[\mathbf{2}]$) (yield 0.27 g, 0.22 mmol, 29% based on $[Et_4N]_2[Se_2Cr_3(CO)_{10}]$). IR ($\nu_{CO}$, CH_2Cl_2): 2048 (m), 1986 (vs), 1977 (s, sh), 1925 (s, br), 1876 (m, br) cm^{-1}. Anal. Calcd for $[Et_4N]_2[\mathbf{2}]$: C, 34.66; H, 3.23; N, 2.25. Found: C, 34.43; H, 3.28; N, 2.20. ICP-AES: Mn: Cr = 1.49: 1. ^{1}H NMR (400 MHz, DMSO-d_6, 300 K): δ 1.15 (br, $-CH_2CH_3$), 3.20 (br, $-CH_2CH_3$). ^{13}C NMR (100 MHz, DMSO-d_6, 300 K): δ 7.55 ($-CH_2CH_3$), 51.9 ($-CH_2CH_3$), 213.7, 216.9, 217.3, 221.0, 225.2 ($-CO$). Crystals of $[Et_4N]_2[\mathbf{2}]$ suitable for X-ray diffraction were grown from Et_2O/CH_2Cl_2. ^{1}H NMR (400 MHz, DMSO-d_6, 300 K) for $[Et_4N]_2[Se_2Cr_3(CO)_{10}]$: δ 1.15 (br, $-CH_2CH_3$), 3.20 (br, $-CH_2CH_3$).

Method 2. An acetone solution (20 mL) of $[Et_4N]_2[Se_2Cr_3(CO)_{10}]$ (0.56 g, 0.66 mmol), $Mn(CO)_5Br$ (0.33 g, 1.20 mmol), and 4 M HCl (1.33 mL) was stirred at 35 °C for 10 h. The solution was filtered, and the solvent was evaporated under vacuum. The residue was washed with hexanes several times and extracted with Et_2O to give a reddish-orange solution that was recrystallized with hexanes/Et_2O to give $[Et_4N][Me_2CSe_2\{Mn(CO)_4\}\{Cr(CO)_5\}_2]$ ($[Et_4N][\mathbf{1}]$) (yield 0.35 g, 0.40 mmol, 61% based on $[Et_4N]_2[Se_2Cr_3(CO)_{10}]$). The residue was extracted with CH_2Cl_2 to give a yellowish-brown solution and then with Et_2O/CH_2Cl_2 to give $[Et_4N]_2[Se_2Mn_3(CO)_{10}\{Cr(CO)_5\}_2]$ ($[Et_4N]_2[\mathbf{2}]$) (yield 0.10 g, 0.08 mmol, 12% based on $[Et_4N]_2[Se_2Cr_3(CO)_{10}]$).

Reaction of $[Et_4N]_2[Se_2Cr_3(CO)_{10}]$ with $Mn(CO)_5Br$ in Butanone. A butanone solution (40 mL) of $[Et_4N]_2[Se_2Cr_3(CO)_{10}]$ (1.11 g, 1.30 mmol) and $Mn(CO)_5Br$ (0.64 g, 2.33 mmol) was stirred at 35 °C for 10 h. The solution was filtered, and the solvent was evaporated under vacuum. The residue was washed with hexanes and Et_2O several times, and extracted with CH_2Cl_2 to give a yellowish-brown solution and then with Et_2O/CH_2Cl_2 to give $[Et_4N]_2[Se_2Mn_3(CO)_{10}\{Cr(CO)_5\}_2]$ ($[Et_4N]_2[\mathbf{2}]$) (yield 0.45 g, 0.36 mmol, 28% based on $[Et_4N]_2[Se_2Cr_3(CO)_{10}]$).

Acidification of $[Et_4N]_2[Se_2Cr_3(CO)_{10}]$ with $Mn(CO)_5Br$ in Butanone. A butanone solution (20 mL) of $[Et_4N]_2[Se_2Cr_3(CO)_{10}]$ (0.48 g, 0.56 mmol), $Mn(CO)_5Br$ (0.28 g, 1.02 mmol), and 4 M HCl (1.33 mL) was stirred at 35 °C for 10 h. The solution was filtered, and the solvent was evaporated under vacuum. The residue was washed with hexanes several times, and extracted with Et_2O to give a reddish-brown solution which was recrystallized with hexanes/Et_2O to give $[Et_4N][Se_2Mn_3(CO)_9]$[10a] (yield 0.15 g, 0.21 mmol, 38% based on $[Et_4N]_2[Se_2Cr_3(CO)_{10}]$).

Reaction of $[Et_4N][Me_2CSe_2\{Mn(CO)_4\}\{Cr(CO)_5\}_2]$ ($[Et_4N][\mathbf{1}]$) with $Mn_2(CO)_{10}$/KOH. To a MeCN solution (20 mL) of $[Et_4N][Me_2CSe_2\{Mn(CO)_4\}\{Cr(CO)_5\}_2]$ ($[Et_4N][\mathbf{1}]$) (0.15 g, 0.17 mmol) was added $Mn_2(CO)_{10}$ (0.07 g, 0.18 mmol) and KOH (0.56 g, 9.98 mmol) in MeOH (5 mL). The mixed solution was stirred for 48 h. The solution was filtered, and the solvent was evaporated under vacuum. The residue was washed with hexanes and Et_2O several times and extracted with CH_2Cl_2 to give a solution which was recrystallized with CH_2Cl_2 and with Et_2O/CH_2Cl_2 to give $[Et_4N]_2[Se_2Mn_3(CO)_{10}\{Cr(CO)_5\}_2]$ ($[Et_4N]_2[\mathbf{2}]$) (yield 0.07 g, 0.06 mmol, 35% based on $[Et_4N][\mathbf{1}]$).

Reaction of $[Et_4N][Me_2CSe_2\{Mn(CO)_4\}\{Cr(CO)_5\}_2]$ ($[Et_4N][\mathbf{1}]$) with $Mn(CO)_5Br$. An acetone solution (15 mL) of $[Et_4N][Me_2CSe_2\{Mn(CO)_4\}\{Cr(CO)_5\}_2]$ ($[Et_4N][\mathbf{1}]$) (0.11 g, 0.12 mmol) and $Mn(CO)_5Br$ (0.06 g, 0.22 mmol) was stirred at 35 °C for 9 h. The solution was filtered, and the solvent was evaporated under vacuum. The residue was washed with hexanes several times and extracted with Et_2O to give a reddish-brown solution which was recrystallized with hexanes/Et_2O to give $[Et_4N][Se_2Mn_3(CO)_9]$[10a] (yield 0.05 g, 0.07 mmol, 58% based on $[Et_4N][\mathbf{1}]$). The residue was then extracted with CH_2Cl_2 to give $[Cr(CO)_5Br]^-$[20] confirmed by IR spectroscopy.

Reaction of $[Et_4N]_2[Se_2Mn_3(CO)_{10}\{Cr(CO)_5\}_2]$ ($[Et_4N]_2[\mathbf{2}]$) with $Mn(CO)_5Br$. An acetone solution (20 mL) of $[Et_4N]_2[Se_2Mn_3(CO)_{10}\{Cr(CO)_5\}_2]$ ($[Et_4N]_2[\mathbf{2}]$) (0.16 g, 0.13 mmol) and $Mn(CO)_5Br$ (0.06 g, 0.22 mmol) was stirred at 35 °C for 18 h. The solution was filtered, and the solvent was evaporated under vacuum. The residue was washed with hexanes several times and extracted with Et_2O to give a reddish-brown solution which was recrystallized with hexanes/Et_2O to give $[Et_4N][Se_2Mn_3(CO)_9]$[10a] (yield 0.05 g, 0.07 mmol, 54% based on $[Et_4N]_2[\mathbf{2}]$). The residue was then extracted with CH_2Cl_2 to give $[Cr(CO)_5Br]^-$[20] confirmed by IR spectroscopy.

Reaction of $[Et_4N]_2[Se_2Mn_3(CO)_{10}\{Cr(CO)_5\}_2]$ ($[Et_4N]_2[\mathbf{2}]$) with CO. Carbon oxide was bubbled through a solution of $[Et_4N]_2[Se_2Mn_3(CO)_{10}\{Cr(CO)_5\}_2]$ ($[Et_4N]_2[\mathbf{2}]$) (0.16 g, 0.13 mmol) in MeCN (20 mL) at 50 °C for 15 min. After stirring for another 12 h at 50 °C, the color of the solution changed from yellowish-brown to reddish-brown. The solution was filtered, and the solvent was evaporated under vacuum. The residue was washed with hexanes that were shown by IR spectroscopy to contain $Cr(CO)_6$. The residue was further extracted with CH_2Cl_2 to give $[Et_4N]_2[Se_2Mn_3(CO)_9]$[13d] (yield 0.07 g, 0.08 mmol, 62% based on $[Et_4N]_2[\mathbf{2}]$). ^{1}H NMR (400 MHz, DMSO-d_6, 300 K, ppm) for $[Et_4N]_2[Se_2Mn_3(CO)_9]$: δ 1.11 (br, $-CH_2CH_3$), 3.32 (br, $-CH_2CH_3$).

X-ray Structural Characterization of $[Et_4N][\mathbf{1}]$ and $[Et_4N]_2[\mathbf{2}]$. Selected crystallographic data for $[Et_4N][\mathbf{1}]$ and $[Et_4N]_2[\mathbf{2}]$ are given in Table 5. All crystals were mounted on glass fibers with epoxy cement. Data collection for $[Et_4N][\mathbf{1}]$ was carried out using a Nonius (CAD-4) diffractometer with graphite-monochromated Mo Kα radiation at 298 K in the 2θ range of 2.0−50° employing $\theta-2\theta$ scans, and an empirical absorption correction by azimuthal (ψ) scans was applied.[28] Data collection for

(28) North, A. C. T.; Philips, D. C.; Mathews, F. S. *Acta Crystallogr.* **1968**, *A24*, 351–358.

Table 5. Crystallographic Data for $[Et_4N][Me_2CSe_2\{Mn(CO)_4\}\{Cr(CO)_5\}_2]$ ($[Et_4N][\mathbf{1}]$) and $[Et_4N]_2[Se_2Mn_3(CO)_{10}\{Cr(CO)_5\}_2]$ ($[Et_4N]_2[\mathbf{2}]$)

	$[Et_4N][\mathbf{1}]$	$[Et_4N]_2[\mathbf{2}]$
empirical formula	$C_{25}H_{26}Cr_2MnNO_{14}Se_2$	$C_{20}Cr_2Mn_3O_{20}Se_2$[a]
Fw	881.33	986.94
cryst syst	triclinic	monoclinic
space group	$P\bar{1}$	$C2/m$
crystal dimens, mm	0.40 × 0.30 × 0.15	0.30 × 0.10 × 0.05
a, Å	9.757(2)	13.4239(5)
b, Å	11.2691(8)	20.1031(8)
c, Å	16.900(6)	9.2313(3)
α, deg	81.77(2)	
β, deg	76.05(3)	98.817(3)
γ, deg	71.590(9)	
V, Å^3	1706.5(7)	2461.7(2)
Z	2	2
D (calcd), g cm^{-3}	1.715	1.332
μ, mm^{-1}	3.185	2.707
diffractometer	Nonius (CAD4)	Nonius (Kappa CCD)
radiation (λ), Å	0.71073	0.71073
temp, K	298(2)	298(2)
θ range for data collecn, deg	1.91−24.92	2.03−25.00
T_{min}/T_{max}	0.37/0.62	0.67/0.72
no. of indep reflns ($I > 2\,\sigma(I)$)	4010 (R_{int} = 0.0188)	1701 (R_{int} = 0.0679)
no. of parameters	385	130
R1[b]/wR2[b]	0.033/0.085 ($I > 2\,\sigma(I)$)	0.050/0.141 ($I > 2\,\sigma(I)$)
R1[b]/wR2[b] (all data)	0.072/0.103	0.067/0.152

[a] Two cationic molecules, Et_4N^+, are excluded in the formula, formula weight, calculated density, μ, and $F(000)$ according to the Platon Squeeze procedure. [b] The functions minimized during least-squares cycles were $R1 = \sum||F_o| - |F_c||/\sum|F_o|$ and $wR2 = [\sum w(F_o^2 - F_c^2)^2/\sum w(F_o^2)^2]^{1/2}$.

$[Et_4N]_2[\mathbf{2}]$ was carried out using a Bruker-Nonius Kappa CCD diffractometer with graphite-monochromated Mo Kα radiation at 298 K employing the $\theta-2\theta$ scan mode, and an empirical absorption correction by multiscans was applied. The structures of $[Et_4N][\mathbf{1}]$ and $[Et_4N]_2[\mathbf{2}]$ were refined by the SHELXL package.[29]

For $[Et_4N][\mathbf{1}]$ and $[Et_4N]_2[\mathbf{2}]$, there are several close inter N···C and C···C contacts because of the disorder which implies disorder of the $[Et_4N]^+$ cations. For $[Et_4N][\mathbf{1}]$, the N1 and N2 atoms on the $[Et_4N]^+$ each reside on a crystallographic inversion center with a site-occupation factor of 0.5. The C18, C20 (on N1 atom), C22, and C24 (on N2 atom) were disordered 50% in the first moiety and 50% for C18′, C20′ (on N1 atom), C22′, and C24′ (on N2 atom). Thus, the C atoms on the disordered cations of $[Et_4N][\mathbf{1}]$ were refined with isotropic temperature factors. For $[Et_4N]_2[\mathbf{2}]$, the final structure of **2** was refined without the two cations, $[Et_4N]^+$, by using the SQUEEZE option of PLATON. Except for the C atoms on the cations of $[Et_4N][\mathbf{1}]$, all of the non-hydrogen atoms for $[Et_4N][\mathbf{1}]$ and **2** were refined with anisotropic temperature factors. Additional crystallographic data in the form of CIF files are available as Supporting Information.

Computational Details. All calculations reported in the present study were performed via the DFT with the exchange and correlation functionals of the gradient correction proposed in 1991 by Perdew and Wang (PW91)[22,23] and with a LanL2DZ basis set using the Gaussian 03 series of packages.[30] The geometry of $[Se_2Cr_3(CO)_{10}]^{2-}$ was taken from single-crystal X-ray diffraction data, and the isopropylene group of complex **1** was replaced by the *sec*-butylene group, forming the proposed structure **1′**. The geometries of **1**, the proposed complex **1′**, **2**, and $[Se_2Mn_3(CO)_9]^{2-}$ were fully optimized with the same level of theory. Wiberg bond indices[24] and natural charges[25] were evaluated using the Weinhold NBO method.[31] Graphical representations of the molecular orbitals and spin densities were obtained using CS Chem3D 5.0.

Acknowledgment. This work was supported by the National Science Council of Taiwan (NSC Grant 98-2113-M-003-006-MY3 to M.S.). We are also grateful to the National Center for High-Performance Computing, where the Gaussian package and computer time were provided.

Supporting Information Available: X-ray crystallographic files in CIF format for $[Et_4N][\mathbf{1}]$ and $[Et_4N]_2[\mathbf{2}]$ and magnetic measurements (PDF) for $[Et_4N]_2[Se_2Cr_3(CO)_{10}]$, $[Et_4N]_2[\mathbf{2}]$, and $[PPN]_2[Se_2Mn_3(CO)_9]$. Computational details for $[Se_2Cr_3(CO)_{10}]^{2-}$, **1**, **1′**, **2**, and $[Se_2Mn_3(CO)_9]^{2-}$. This material is available free of charge via the Internet at http://pubs.acs.org.

(29) Sheldrick, G. M. *SHELXL97*, version 97-2; University of Göttingen: Göttingen, Germany, 1997.

(30) Frisch, M. J.; Trucks, G. W.; Schlegel, H. B.; Scuseria, G. E.; Robb, M. A.; Cheeseman, J. R.; Montgomery, J. A., Jr.; Vreven, T.; Kudin, K. N.; Burant, J. C.; Millam, J. M.; Iyengar, S. S.; Tomasi, J.; Barone, V.; Mennucci, B.; Cossi, M.; Scalmani, G.; Rega, N.; Petersson, G. A.; Nakatsuji, H.; Hada, M.; Ehara, M.; Toyota, K.; Fukuda, R.; Hasegawa, J.; Ishida, M.; Nakajima, T.; Honda, Y.; Kitao, O.; Nakai, H.; Klene, M.; Li, X.; Knox, J. E.; Hratchian, H. P.; Cross, J. B.; Bakken, V.; Adamo, C.; Jaramillo, J.; Gomperts, R.; Stratmann, R. E.; Yazyev, O.; Austin, A. J.; Cammi, R.; Pomelli, C.; Ochterski, J. W.; Ayala, P. Y.; Morokuma, K.; Voth, G. A.; Salvador, P.; Dannenberg, J. J.; Zakrzewski, V. G.; Dapprich, S.; Daniels, A. D.; Strain, M. C.; Farkas, O.; Malick, D. K.; Rabuck, A. D.; Raghavachari, K.; Foresman, J. B.; Ortiz, J. V.; Cui, Q.; Baboul, A. G.; Clifford, S.; Cioslowski, J.; Stefanov, B. B.; Liu, G.; Liashenko, A.; Piskorz, P.; Komaromi, I.; Martin, R. L.; Fox, D. J.; Keith, T.; Al-Laham, M. A.; Peng, C. Y.; Nanayakkara, A.; Challacombe, M.; Gill, P. M. W.; Johnson, B.; Chen, W.; Wong, M. W.; Gonzalez, C.; Pople, J. A. *Gaussian 03*, Revision B.04; Gaussian, Inc.: Wallingford, CT, 2004.

(31) Reed, A. E.; Curtiss, L. A.; Weinhold, F. *Chem. Rev.* **1988**, *88*, 899–926.